

## Supplementary Material

### Non-invasive imaging of PARP1 expression in glioblastoma models

#### Journal: Molecular Imaging and Biology

Brandon Carney,<sup>1,2,#</sup> Giuseppe Carlucci,<sup>1,#</sup> Beatriz Salinas,<sup>1</sup> Valentina Di Gialleonardo,<sup>1</sup>  
Susanne Kossatz,<sup>1</sup> Axel Vansteene,<sup>1</sup> Valerie A Longo,<sup>1</sup> Alexander Bolaender,<sup>3</sup> Gabriela  
Chiosis,<sup>3</sup>  
Kayvan R Keshari,<sup>1,3,4</sup> Wolfgang A Weber,<sup>1,3,4</sup> Thomas Reiner<sup>1,4,\*</sup>

<sup>1</sup> Department of Radiology, Memorial Sloan Kettering Cancer Center, New York, NY 10065,  
USA

<sup>2</sup> Ph.D. Program in Chemistry, The Graduate Center of the City University of New York,  
NY 10018, USA

<sup>3</sup> Program in Molecular Pharmacology, Memorial Sloan Kettering Cancer Center, New York,  
NY 10065, USA

<sup>4</sup> Weill Cornell Medical College, New York, NY 10065, USA

## Table of Contents

<b>MATERIALS AND METHODS</b> .....	<b>2</b>
Cell culture .....	2
Mouse models.....	3
PARP-1 Immunohistochemistry.....	3
Synthesis of [ <sup>19</sup> F]PARPi .....	4
Radiosynthesis of [ <sup>18</sup> F]PARPi .....	4
IC <sub>50</sub> Determination .....	5
Chromatographic Hydrophobicity Index (logP <sub>CHI</sub> ).....	5
Octanol–Water Partition Coefficient (logP <sub>OW</sub> ) .....	5
Plasma Protein Binding .....	6
PARPi-FL Blocking Studies.....	6
Blood Half-Life .....	6
Blood Stability .....	7
Autoradiography and Hematoxylin–Eosin staining .....	7
Ex vivo biodistribution.....	7
PET/CT imaging .....	8
PET/MRI imaging .....	8
<b>SUPPLEMENTARY FIGURES</b> .....	<b>10</b>
Figure S1. Analytical characteristics of [ <sup>19</sup> F]PARPi. ....	10
Figure S2. Stability of [ <sup>18</sup> F]PARPi as determined by HPLC. ....	10
Figure S3. Stability of [ <sup>18</sup> F]PARPi as determined by HPLC. ....	12
Table S1. Ex vivo biodistribution of [ <sup>18</sup> F]PARPi. ....	13
Figure S4. PARP1 expression of a murine popliteal lymph node.....	14
Figure S5. Expression in normal mouse tissues.....	15
Figure S6. PET Imaging. ....	16
Figure S7. PARP1 expression in an orthotopic glioblastoma model. ....	17
<b>REFERENCES</b> .....	<b>18</b>

## **MATERIALS AND METHODS**

Commercially available compounds were used without further purification unless otherwise stated. 4,7,13,16,21,24-Hexaoxa-1,10-diazabicyclo[8.8.8]hexacosane ( $K_{222}$ ) was purchased from Sigma Aldrich (St. Louis, MO). Extra dry dimethyl sulfoxide (DMSO) over molecular sieves was purchased from Acros Organics (Geel, Belgium). Water ( $>18.2 \text{ M}\Omega\text{cm}^{-1}$  at  $25 \text{ }^\circ\text{C}$ ) was obtained from an Alpha-Q Ultrapure water system from Millipore (Bedford, MA). Olaparib (AZD2281) was purchased from LC Laboratories (Woburn, MA). PARPi-FL was synthesized as described earlier (1). No-carrier-added (n.c.a.) [ $^{18}\text{F}$ ]fluoride was obtained via the  $^{18}\text{O}(\text{p},\text{n})^{18}\text{F}$  nuclear reaction of 16.5-MeV protons in an GE Healthcare PETTrace 800 using enriched  $^{18}\text{O}$ -water. QMA light ion-exchange cartridges and C-18 light Sep-Pak® cartridges were obtained from Waters (Milford, MA). High performance liquid chromatography (HPLC) purification and analysis was performed on a Shimadzu UFLC HPLC system equipped with a DGU-20A degasser, a SPD-M20A UV detector, a LC-20AB pump system, and a CBM-20A communication BUS module. A LabLogic Scan-RAM radio-TLC/HPLC-detector was used for the radioactive signal. HPLC solvents (Buffer A: 0.1% TFA in water, Buffer B: 0.1% TFA in MeCN) were filtered before use. HPLC analysis and purification was performed on a reversed phase Phenomenex Gemini column (C6-Phenyl,  $5 \mu\text{m}$ ,  $4.6 \text{ mm}$ ,  $250 \text{ mm}$ ). Analysis was performed with Method A (flowrate:  $1.5 \text{ mL/min}$ ; gradient: 0-14 min 5-100% B; 14-17.5 min 100% B; 17.5-18 min 100%-5% B); purification was performed with Method B (flowrate:  $1.5 \text{ mL/min}$ ; isocratic: 0-14 min 5-100% B; 14-17.5 min 100% B; 17.5-18 min 100%-5% B). Electrospray ionization mass spectrometry (ESI-MS) spectra were recorded with a Shimadzu LC-2020 with electrospray ionization SQ detector. All PET imaging experiments were conducted on a microPET INVEON camera equipped with a CT scanner (Siemens, Knoxville, TN). Digital phosphor autoradiography of orthotopic U251 MG tumors with surrounding brain tissue as well as muscle were obtained using a Typhoon FLA 7000 laser scanner from GE Healthcare (Port Washington, NY).

### **Cell culture**

The human glioblastoma cell lines U251 MG and U373 MG were kindly provided by the Laboratory of Dr. Ronald Blasberg (MSKCC, New York, NY). Cell lines were grown in Eagle's Minimal Essential Medium (MEM), 10% (vol/vol) heat inactivated fetal bovine serum,  $100 \text{ IU}_2$

penicillin, and 100 µg/mL streptomycin, purchased from the culture media preparation facility at MSKCC (New York, NY).

### **Mouse models**

All animal experiments were done in accordance with protocols approved by the Institutional Animal Care and Use Committee of MSKCC and followed National Institutes of Health guidelines for animal welfare. Female athymic nude CrTac:NCr-Foxn1nu mice at age 6 - 8 weeks were purchased from Taconic Laboratories (Hudson, NY). Non tumor-bearing mice were used to determine the blood half-life of [<sup>18</sup>F]PARPi (n = 3). Xenograft mouse models were used to determine the pharmacokinetics (n = 12). For subcutaneous injections, mice were anesthetized with 2% isoflurane (Baxter Healthcare) (2 l/min medical air). U251 MG cells were implanted subcutaneously ( $5 \times 10^6$  cells in 150 µL 1:1 PBS/matrigel® (BD Biosciences, San Jose, CA) in the right shoulder and allowed to grow for approximately two weeks until the tumors reached 5–10 mm in diameter. For orthotopic injections, mice were anesthetized with 2% isoflurane (Baxter Healthcare) (2 L/min medical air). U251 MG cells ( $5 \times 10^5$  cells in 2 µL PBS) were injected 2 mm lateral and 1 mm anterior to the bregma using a Stoelting Digital New Standard Stereotaxic Device and a 5 µL Hamilton syringe. Cells were allowed to grow for approximately three weeks. For all intravenous injections, mice were gently warmed with a heat lamp and placed on a restrainer. The tails were sterilized with alcohol pads, and injection took place via the lateral tail vein.

### **PARP-1 Immunohistochemistry**

Immunohistochemical staining of PARP-1 was performed on 3 µm section, obtained from with formalin-fixed, paraffin-embedded tumor-bearing and normal mouse brain using the Discovery XT processor (Ventana Medical Systems, Tucson, AZ) at the Molecular Cytology Core Facility of MSKCC. Following deparaffinization with EZPrep buffer and antigen retrieval with CC1 buffer (both Ventana Medical Systems), sections were blocked for 30 minutes with Background Buster solution (Innovex, Lincoln, RI). Primary rabbit anti-PARP-1 antibody (sc-7150, 0.4 µg/mL, Santa Cruz, Dallas, TX) was incubated for 5 hours followed by a biotinylated goat anti-rabbit IgG for 1 h (PK6101, 1:200 Vector labs, Burlingame, CA). Signal detection was performed with a DAB<sub>3</sub>

detection kit (Ventana Medical Systems, Tucson, AZ) according to the manufacturer's instructions. Sections were counterstained with hematoxylin and coverslipped with Permount (Fisher Scientific, Waltham, MA). Adjacent sections were stained with Hematoxylin and Eosin for morphological evaluation of the tissue.

### Synthesis of [<sup>19</sup>F]PARPi

4-(4-fluoro-3-(piperazine-1-carbonyl)benzyl)phthalazin-1(2H)-one was synthesized as previously described (2). To 20 mg (54.5 μmol) of 4-(4-fluoro-3-(piperazine-1-carbonyl)benzyl)phthalazin-1(2H)-one dissolved in 1 mL of MeCN, 9.2 mg (65.5 μmol) 4-fluorobenzoic acid was added followed by 24.8 mg (65.5 μmol) of N,N,N',N'-Tetramethyl-O-(1H-benzotriazol-1-yl)uronium hexafluorophosphate (HBTU) and 18 μL (131 μmol) of Et<sub>3</sub>N. The reaction mixture was stirred for 5 minutes and purified by HPLC to yield the compound as an orange solid (11.5 mg, 23.5 μmol, 43%). <sup>1</sup>H-NMR (500 MHz, CDCl<sub>3</sub>) δ = 10.74 (s, 1H), 8.51-8.49 (d, 1H), 7.83-7.76 (m, 2H), 7.82 (s, 1H), 7.45-7.44 (m, 2H), 7.38-7.36 (m, 2H), 7.14-7.08 (m, 3H), 4.33 (s, 2H), 3.75-3.39 (m, 8H). MS-ESI m/z [M + Na]<sup>+</sup> = 511.2. HRMS-ESI m/z calculated for [C<sub>27</sub> H<sub>22</sub> N<sub>4</sub> O<sub>3</sub> F<sub>2</sub> Na]<sup>+</sup> 511.1558, found 511.1569 [M + Na]<sup>+</sup>.

### Radiosynthesis of [<sup>18</sup>F]PARPi

A QMA cartridge containing cyclotron-produced [<sup>18</sup>F] fluoride ion was eluted with a solution containing 9mg Kryptofix [2.2.2] (4,7,13,16,21,24-hexaoxa-1,10-diazabicyclo[8.8.8]hexacosane), 0.08 mL 0.15 M K<sub>2</sub>CO<sub>3</sub> and 1.92 mL MeCN into a 5 mL reaction vial. Water was removed azeotropically at 120 °C. 500 μg of ethyl 4-nitrobenzoate dissolved in 100 μL of DMSO was then added to the reaction vial and heated to 150 °C for 15 minutes. The reaction vial was then allowed to cool as 50 μL of 1M NaOH was added. The reaction mixture was stirred for 1 min and 50 μL of 1M HCl was added to quench. Then, 2 mg of 4-(4-fluoro-3-(piperazine-1-carbonyl)benzyl)phthalazin-1(2H)-one dissolved in 100 μL of DMSO was added followed by 10 mg of HBTU dissolved in 100 μL of DMSO and 20 μL of Et<sub>3</sub>N. The reaction mixture was stirred for 1 minutes. 400 μL MeCN followed by 700 μL H<sub>2</sub>O was then added and the solution was injected onto a C6-Phenyl analytical HPLC column and eluted under isocratic conditions (Method B). [<sup>18</sup>F]PARPi eluted at (t<sub>R</sub> = 25.5 min), which was well resolved from the nitro analogue (4-(4-fluoro-3-(4-(4-nitrobenzoyl)piperazine-1-carbonyl)benzyl)phthalazin-1(2H)-one;<sub>4</sub>

$t_R = 30.1$  min). For intravenous administration, the product-containing fraction was passed through a C18 light-SepPak® cartridge preconditioned with EtOH (10 mL) and water (10 mL). The cartridge was washed with water (3 mL) and [ $^{18}\text{F}$ ]PARPi was eluted using EtOH (400  $\mu\text{L}$ ). The solution was then diluted with 0.9% saline to 10% EtOH. The radiochemical purity of the final formulation was confirmed using analytical HPLC. Coelution with nonradioactive F-19 reference compound confirmed the identity of the radiotracer. To measure radiochemical and chemical purity (>99%), [ $^{18}\text{F}$ ]PARPi was reinjected onto an analytical C6-Phenyl column (gradient A;  $t_R = 11.4$  min).

### **IC<sub>50</sub> Determination**

A commercially available colorimetric assay (Trevigen, Gaithersburg, MD) was used to measure PARP-1 activity in vitro in the presence of varying concentrations of [ $^{19}\text{F}$ ]PARPi. Three-fold dilutions of [ $^{19}\text{F}$ ]PARPi (final concentrations ranging from 1  $\mu\text{M}$  to 33 pM) were incubated with 0.5 U of PARP high specific activity (HSA) enzyme for 10 minutes in histone-coated 96-well plates. All experiments were carried out in triplicate. Positive control samples did not contain inhibitor, and background measurement samples did not contain PARP-1. All reaction mixtures were adjusted to a final volume of 50  $\mu\text{L}$  and a final concentration of 2% dimethyl sulfoxide (DMSO) in assay buffer. The remainder of the assay was performed according to the manufacturer's instructions. PARP-1 activity was measured by absorbance at 450 nm in each well using a Molecular Devices SpectraMax M5 microplate reader (Molecular Devices, Sunnyvale, CA).

### **Chromatographic Hydrophobicity Index (logP<sub>CHI</sub>)**

The Chemical Hydrophobicity Indices (CHI) were measured using a previously developed procedure (3). Briefly, reverse phase HPLC was used to measure the retention times of a set of standards with known CHI. A standard curve was then created to calculate the CHI of [ $^{19}\text{F}$ ]PARPi based on the HPLC retention time.

### **Octanol–Water Partition Coefficient (logP<sub>ow</sub>)**

The lipophilicity of the [ $^{18}\text{F}$ ]PARPi was acquired by adding 2.5  $\mu\text{Ci}$  to a mixture of 0.5 mL of 1-octanol and 0.5 mL of 25 mM phosphate buffered saline (pH 7.4) and mixed for 5 minutes.<sup>5</sup>

Then, the mixture was centrifuged at 15000 rpm for 5 minutes. 100  $\mu$ L samples were obtained from organic and aqueous layers, and the radioactivity of the samples were measured in a  $\gamma$ -counter WIZARD<sup>2</sup> automatic  $\gamma$ -counter (PerkinElmer, Boston, MA). The experiment was performed in triplicate, and the resulting logP<sub>ow</sub> was calculated as the mean  $\pm$  SD.

### **Plasma Protein Binding**

The plasma protein fraction was determined using the Rapid Equilibrium Dialysis Device System (Life Technologies, Grand Island, NY) according to the manufacturer's protocol. Membrane dialysis was performed with 500  $\mu$ M [<sup>19</sup>F]PARPi in serum (500  $\mu$ L) on one side of the membrane and PBS (700  $\mu$ L) on the other side. The system was sealed with parafilm and incubated for 4 h at 37 °C on an orbital shaker set to 100 rpm. Thereafter, 50  $\mu$ L of solution was taken from both sides, and samples were treated with 300  $\mu$ L of precipitation buffer (90/10 acetonitrile/water with 0.1% formic acid) and vortexed to remove protein before HPLC analysis. After injection, the [<sup>18</sup>F]PARPi peaks from each sample were integrated, and the protein bound fraction determined as %bound= [1 – (Concentration buffer chamber/Concentration plasma chamber)] $\times$ 100. The final Albumin binding was calculated as the mean  $\pm$  SD.

### **PARPi-FL Blocking Studies**

U251 MG or U373 MG ( $1 \times 10^4$  cells per well) cells were seeded into 12 wells each on a 96-well plate and cultured for 24 hours. The cells were then incubated either alone, with PARPi-FL (500 nM), or with PARPi-FL (500 nM) and Olaparib or [<sup>19</sup>F]PARPi in 10-fold excess (5  $\mu$ M) at 37 °C for 30 minutes. Experiments were performed in triplicate. Following incubation, cells were washed twice with media and twice with PBS and imaged with a Zeiss LSM 5Live confocal microscope. Images were then quantified using ImageJ 1.47u processing software.

### **Blood Half-Life**

The blood half-life of [<sup>18</sup>F]PARPi was calculated by measuring the activity of blood samples collected at different time points p.i. (5, 15, 30, 45, 60, 90 and 120 minutes). Female nude mice (n = 3) were injected via lateral tail vein with [<sup>18</sup>F]PARPi (50  $\mu$ Ci in 200  $\mu$ L 10% EtOH in 0.9% sterile saline) and blood samples were collected from the great saphenous vein of each animal at the predetermined time point. The collected blood was weighed and counted in a WIZARD<sup>2</sup><sub>6</sub>

automatic  $\gamma$ -counter (PerkinElmer, Boston, MA). The blood half-life was calculated using Prism 6.0c (GraphPad Software, La Jolla, CA) using a two-phase decay least squares fitting method and expressed as %ID/g.

### **Blood Stability**

[ $^{18}\text{F}$ ]PARPi (approximately 200  $\mu\text{Ci}$ , 45  $\text{mCi}/\mu\text{mol}$  in 200  $\mu\text{L}$ , 10% EtOH in 0.9% sterile saline) was added to 250  $\mu\text{L}$  of whole human blood and incubated at 37  $^{\circ}\text{C}$  for increasing lengths of time (15, 30, 60, 120 and 240 minutes). [ $^{18}\text{F}$ ]PARPi was then extracted with 750  $\mu\text{L}$  of MeCN, then centrifuged (5 minutes at 5000 rpm) to pellet blood cells and proteins. The supernatant was collected and prepared for HPLC injection by adding 750  $\mu\text{L}$  mQ  $\text{H}_2\text{O}$  and filtering. The blood stability was measured by HPLC analysis (Method A).

### **Autoradiography and Hematoxylin–Eosin staining**

One day after PET/CT imaging, the same orthotopic U251 MG tumor bearing mice were administered with [ $^{18}\text{F}$ ]PARPi (80  $\mu\text{Ci}$ , 45  $\text{mCi}/\mu\text{mol}$  in 300  $\mu\text{L}$  10% EtOH in 0.9% sterile saline) via tail vein injection. Blocked mice from the previous day received another dose of Olaparib (37  $\text{mM}$ , 3.7  $\mu\text{mol}$ , about 80  $\text{mg}/\text{kg}$ , in 100  $\mu\text{L}$  15% PEG<sub>300</sub> / 85% 0.9% saline). The mice were sacrificed after 2 hours and brain and muscle tissues harvested. The collected organs were fixed in Tissue-Tek O.C.T. compound (Sakura Finetek, Torrance, CA) and flash-frozen in liquid nitrogen and cut into 20  $\mu\text{m}$  sections using a Vibratome UltraPro 5000 Cryostat (Vibratome, St. Louis, MO). A storage phosphor autoradiography plate (Fujifilm, BAS-MS2325, Fuji Photo Film, Japan) was exposed to the tissue slices overnight at -20  $^{\circ}\text{C}$  and read the following day. Relative count intensity of the sections in each image was quantified using ImageJ 1.47u processing software. Tumor/muscle and brain/muscle ratios were calculated using Prism 6.0c (GraphPad Software, La Jolla, CA). The same sections were subsequently subjected to H&E staining (hematoxylin–eosin) for morphological evaluation of tissue pathology and to compare the localization of the radiotracer with the location of tumor tissue.

### **Ex vivo biodistribution**

Biodistribution studies were performed in subcutaneous U251 MG xenograft bearing athymic nude mice ( $n = 12$ ). Mice were divided in two groups (blocked and unblocked) and<sub>7</sub>



administered with [ $^{18}\text{F}$ ]PARPi (approximately 50  $\mu\text{Ci}$ , 45  $\text{mCi}/\mu\text{mol}$  in 200  $\mu\text{L}$ , 10% EtOH in 0.9% sterile saline) via tail vein injection. The blocked group was pre-injected 30 min prior with a 500-fold excess of Olaparib (18 mM, 2  $\mu\text{mol}$ , about 40 mg/kg, in 100  $\mu\text{L}$  15% PEG<sub>300</sub> / 85% 0.9% saline). Mice were sacrificed by CO<sub>2</sub> asphyxiation at 120 min p.i. and major organs were collected, weighed, and counted in a WIZARD<sup>2</sup> automatic  $\gamma$ -counter (PerkinElmer, Boston, MA). The radiopharmaceutical uptake was expressed as a percentage of injected dose per gram (%ID/g) using the following formula: [(activity in the target organ/grams of tissue)/injected dose] $\times$ 100%.

### **PET/CT imaging**

Mice bearing orthotopic U251 MG (n = 8) were divided in two groups (unblocked and blocked) and administered with [ $^{18}\text{F}$ ]PARPi (150  $\mu\text{Ci}$ , 45  $\text{mCi}/\mu\text{mol}$  in 300  $\mu\text{L}$  10% EtOH in 0.9% sterile saline) via tail vein injection. The blocked cohort (n = 4) was pre-injected with Olaparib (37 mM, 3.7  $\mu\text{mol}$ , about 80 mg/kg, in 100  $\mu\text{L}$  15% PEG300 / 85% 0.9% saline) 30 min prior to injection of [ $^{18}\text{F}$ ]PARPi. Approximately 5 min prior to PET acquisition, mice were anesthetized by inhalation of a mixture of isoflurane (Baxter Healthcare, Deerfield, IL, USA; 2% isoflurane, 2 l/min medical air) and positioned on the scanner bed. Anesthesia was maintained using a 1% isoflurane/O<sub>2</sub> mixture. PET data for each mouse was recorded using static scans of 10 minutes and acquired at 30 and 120 minutes post injection. Quantification and %ID/g values were calculated by manually drawing regions of interests in three different frames and determining the average values using ASI Pro VM<sup>TM</sup> MicroPET Analysis software (Siemens Medical Solutions, Knoxville, TX).

### **PET/MRI imaging**

[ $^{18}\text{F}$ ]-PARPi PET images were acquired on integrated in-line preclinical whole-body 1T PET/MRI system (Mediso, Budapest, Hungary). The animals were injected with 200  $\mu\text{Ci}$  of [ $^{18}\text{F}$ ]-PARPi and a 20 minutes static PET scan was acquired 2 hours post injection. 200  $\mu\text{L}$  of diluted gadopentate dimegumine in saline solution (1:5) (Magnevist®; Bayer Pharma, Wayne, NJ) was administered intravenously one minute prior to MRI acquisition. Tumor regions were identified on anatomic images acquired using a post-contrast T<sub>1</sub>-weighted spin-echo (SE) acquisition (T<sub>E</sub>/T<sub>R</sub> = 12.4/671 ms, 0.3125 x 0.3125 mm in plane resolution and 1 mm slice thickness). 30<sub>8</sub>

slices were acquired in order to cover the mouse. Data analysis and PET/MRI co-registration was performed using VivoQuant™ software (inviCro LLC, Boston, USA).

### **Statistical analysis**

All data are expressed as mean  $\pm$  SD. Differences between mouse cohorts were analyzed with the 2-sided unpaired Student test and were considered statistically significant when  $P < 0.05$ .

## SUPPLEMENTARY FIGURES

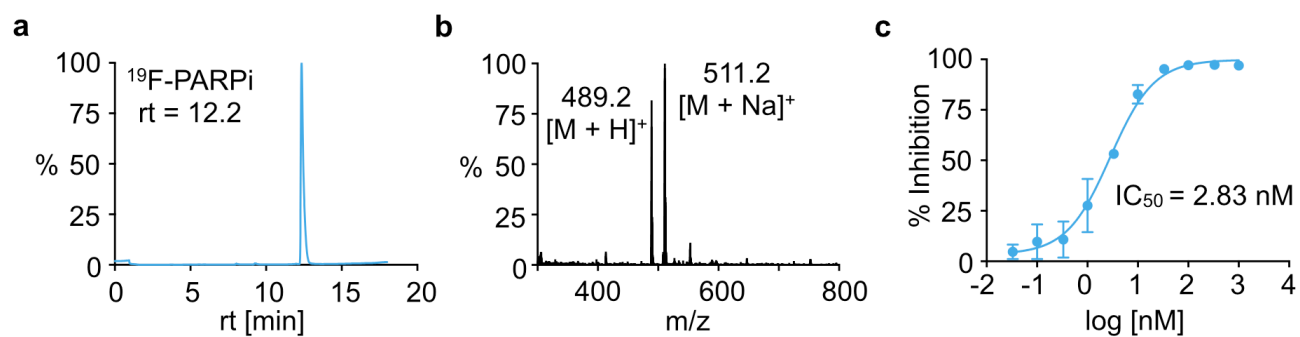


**Fig. S1 Analytical characteristics of  $[^{19}\text{F}]\text{PARPi}$ .** (a) Representative HPLC absorbance trace of  $[^{19}\text{F}]\text{PARPi}$  (b) Positive polarity ESI-MS for  $[^{19}\text{F}]\text{PARPi}$  following purification and (c)  $\text{IC}_{50}$  curve against PARP1 (n = 3).

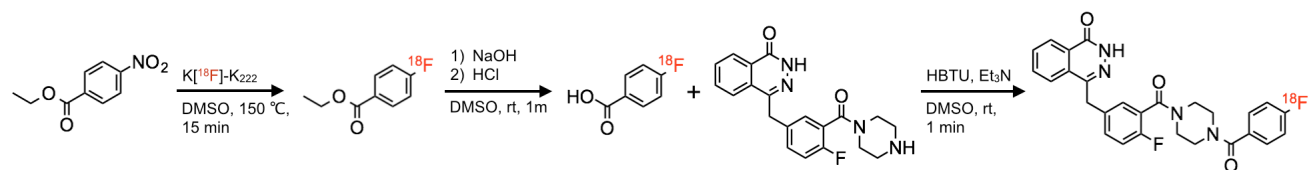


**Fig. S2 Radiochemical synthesis of [<sup>18</sup>F]PARPi.** The total synthesis was realized in a 3 step straightforward strategy. The decay corrected radiochemical yield for the final step was 35%. The total synthesis time from cyclotron to formulation was 90 minutes and the overall uncorrected radiochemical yield was 10% with a specific activity of 48 mCi/ $\mu$ mol.

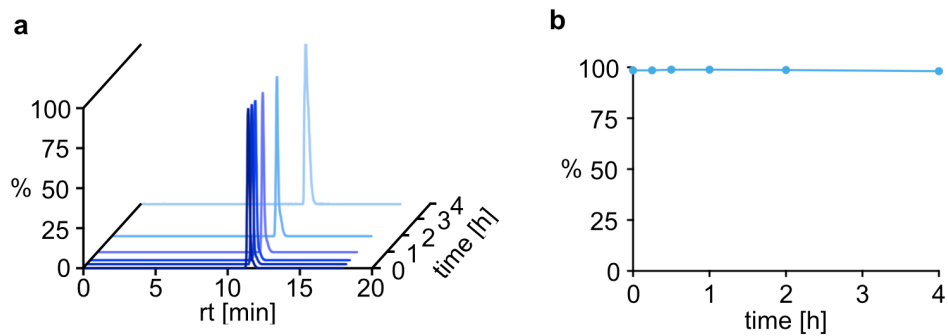


**Fig. S3 Stability of [ $^{18}\text{F}$ ]PARPi as determined by HPLC.** (a) Chromatograms were acquired at different time points (0.25, 0.5, 1, 2 and 4 hours) following incubation at 37 °C. (b) [ $^{18}\text{F}$ ]PARPi fractions were collected and plotted as % of the area of pure compound.

Organ	<sup>18</sup> F]PARPi		Olaparib/ <sup>18</sup> F]PARPi	
	%ID/g	S.D.	%ID/g	S.D.
Tumor	1.82	0.21	0.23	0.09
Heart	0.30	0.08	0.12	0.03
Lung	0.44	0.11	0.38	0.07
Blood	0.41	0.09	0.45	0.36
Liver	3.98	0.56	3.61	2.04
Spleen	4.04	1.23	0.26	0.09
Pancreas	1.71	0.41	0.48	0.25
Kidney	1.17	0.46	0.47	0.22
S I	2.94	0.91	2.35	0.7
L I	2.24	0.59	1.73	0.8
Stomach	0.73	0.3	1.05	0.58
Bone	1.21	0.24	0.21	0.1
Muscle	0.37	0.09	0.19	0.08
Brain	0.04	0.01	0.04	0.03
Lymph Nodes	2.80	0.51	0.13	0.03

**Tab. S1. Ex vivo biodistribution of <sup>18</sup>F]PARPi.** <sup>18</sup>F]PARPi biodistribution was determined in U251 MG xenograft mouse models sacrificed 120 min post injection. Blocking was assessed after injection of a 500-fold excess of Olaparib 30 minutes prior to <sup>18</sup>F]PARPi (n = 6 per group). Values are plotted as %ID/g. SD represents standard deviation.

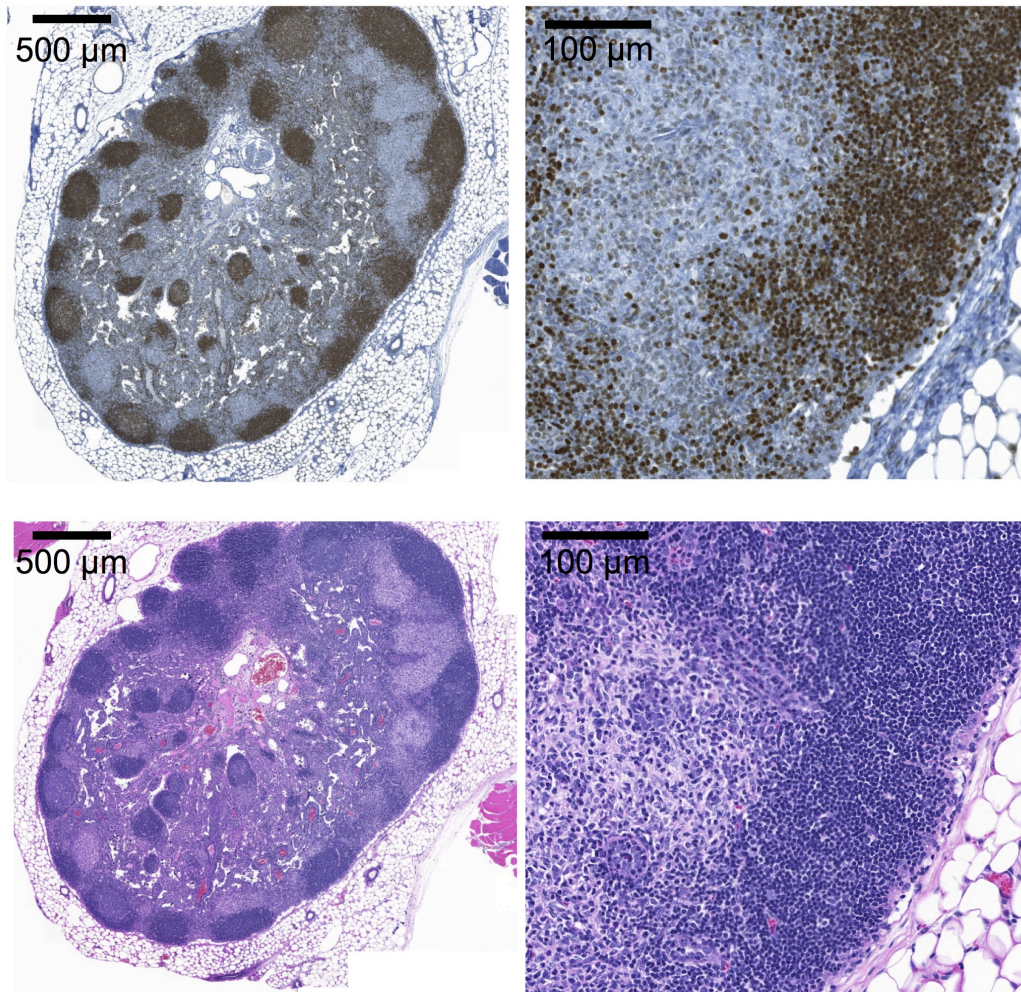


**Fig. S4 PARP1 expression of a murine popliteal lymph node.** PARP1 staining of a mouse lymph node (popliteal lymph node in this case) with corresponding H&E staining. The PARP1 expression was prominently elevated in the follicles. PARP1 immunohistochemical staining was conducted on formalin-fixed, paraffin-embedded tissue derived from nude mice using an anti-PARP antibody and IHC detection. Brown=PARP1 positive tissue. Blue=Hematoxylin counterstain. Red: Eosin stain.

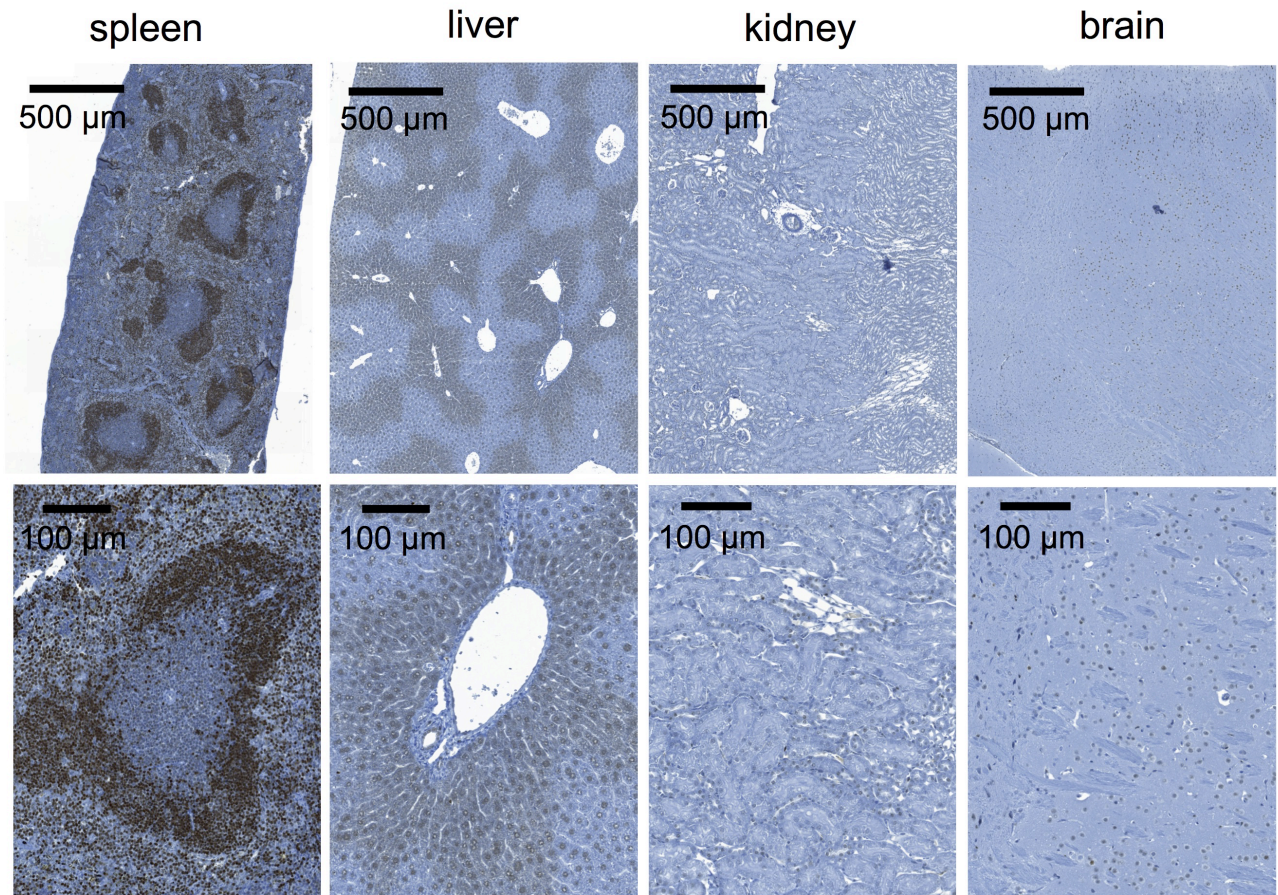


**Fig. S5 Expression in normal mouse tissues.** PARP1 staining of mouse organs (spleen, liver, kidney, brain) to assess inherent PARP1 expression. A high PARP1 expression could be observed in the spleen, particularly around the germinal centers. The other organs did not show prominent nuclear PARP1 staining. PARP1 immunohistochemical staining was conducted on formalin-fixed, paraffin-embedded tissue derived from B6 mice using an anti-PARP antibody and IHC detection. Brown=PARP1 positive tissue. Blue=Hematoxylin counterstain.



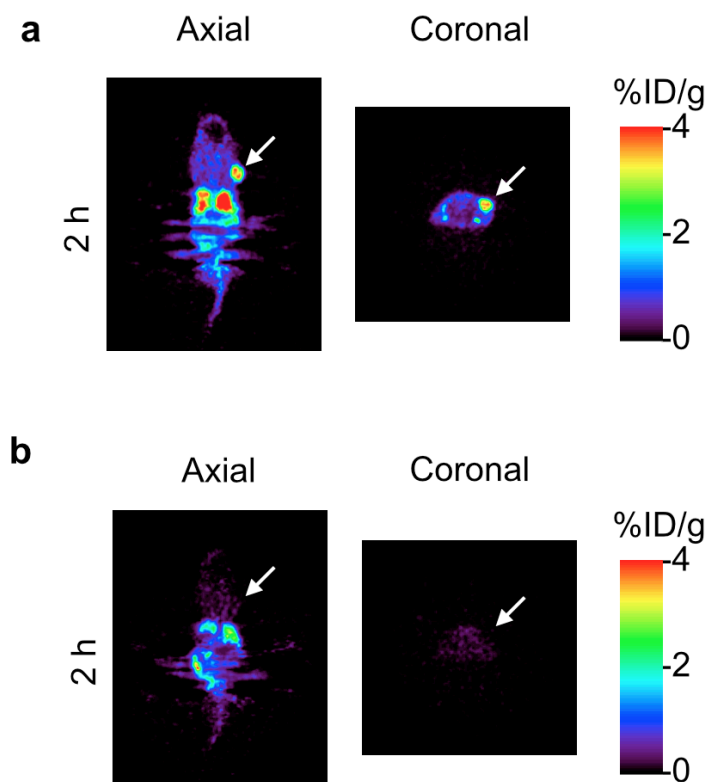


**Fig. S6 PET Imaging.** Coronal and axial PET images of subcutaneous U251 MG bearing mice at 2 hours post injection of (a) [ $^{18}\text{F}$ ]PARPi, or (b) Olaparib/[ $^{18}\text{F}$ ]PARPi injection (500-fold excess of Olaparib, 30 min ahead of radiotracer injection). White arrows point towards tumor xenografts.

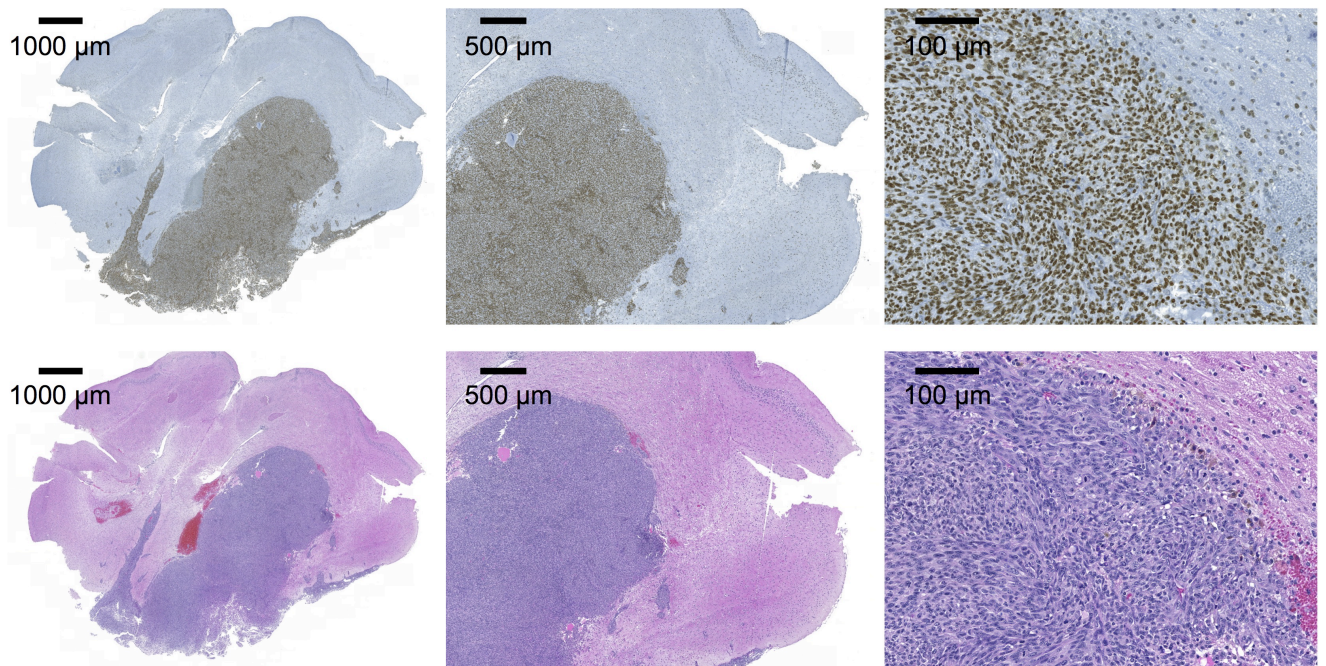


**Fig. S7 PARP1 expression in an orthotopic glioblastoma model.** PARP1 staining of a mouse brain bearing an orthotopic U251 MG glioblastoma with corresponding H&E staining. The PARP1 expression was strongly elevated in the area of the tumor growth with clear margins to surrounding normal brain tissue. PARP1 immunohistochemical staining was conducted on formalin-fixed, paraffin-embedded mouse brains of nude mice using an anti-PARP antibody and IHC detection. Brown=PARP1 positive tissue. Blue=Hematoxylin counterstain. Red: Eosin stain.

## REFERENCES

1. Reiner T, Lacy J, Keliher EJ, et al (2012) Imaging Therapeutic PARP Inhibition In Vivo through Bioorthogonally Developed Companion Imaging Agents. *Neoplasia* 14:169–177
2. Menear KA, Adcock C, Boulter R, et al (2008) 4-[3-(4-cyclopropanecarbonylpiperazine-1-carbonyl)-4-fluorobenzyl]-2H-phthalazine-1-one: a novel bioavailable inhibitor of poly(ADP-ribose) polymerase-1. *J Med Chem* 51:6581–6591
3. Valko K, Bevan C, Reynolds D (1997) Chromatographic Hydrophobicity Index by Fast-Gradient RP-HPLC: A High-Throughput Alternative to log P/log D. *Anal Chem* 69:2022–2029